JOURNAL OF APPLIED ELECTROCHEMISTRY 26 (1996) 803–814

Arsenic poisoning effects on cathodic polarization and hydrogen adsorption at platinum and steel electrodes in KF · 2HF melts

L. J. GAO, S. Y. QIAN, B. E. CONWAY

Department of Chemistry, University of Ottawa, 10 Marie Curie Street, Ottawa, Canada, K1N 6N5

Received 14 August 1995; revised 17 January 1996

It is demonstrated how the presence of arsenic species in the KF · 2HF melt employed as the electrolyte in fluorine production cells greatly affects the electrocatalytic behaviour of the steel electrodes that are used as cathodes. Effects of the introduction of As_2O_3, AsF_3 and AsF_5 as the sources of catalyst poison species have been studied. Such species influence the electrode kinetics of the cathodic hydrogen evolution reaction (h.e.r.) and the adsorption of the overpotential-deposited (o.p.d.) H intermediate. Using Pt, as a model electrocatalyst surface, these effects were quantitatively studied by means of potential–relaxation transients, Tafel relations and cyclic voltammetry, the latter enabling changes of underpotential-deposited C (u.p.d.) H coverage due to the presence of As species to be evaluated. By means of simulation of the potential–relaxation behaviour, information on rate constants, coverages by o.p.d. H and As species were also derived. The presence of As at Pt cathodes suppresses the u.p.d. H adsorption and modifies the o.p.d. H behaviour and the associated pseudocapacitance. The presence and generation of As(–III) species, as AsH_3, in the evolved hydrogen gas was demonstrated by means of Marsh's test. The contact-angles of hydrogen bubbles generated in the h.e.r. at mild-steel electrode surfaces were also determined comparatively in relation to observed sluggish hydrogen bubble detachment from the electrode surfaces when As species were present. *Ex situ* XPS analysis confirmed the presence of As species on the electrode surface.

1. Introduction

The present paper describes new and extended work on processes connected with electrochemical fluorine production from KF · 2HF melts. Previous papers from this laboratory on this topic are referenced in [1–3]. Here we report adsorption and kinetic studies on the hydrogen evolution reaction (h.e.r.) at mild steel electrodes, which are commercially used as cathodes in fluorine-production cells, and at Pt as a model electrocatalyst surface, subject to the effects of the presence of As in the melt acting as a catalyst poison for the h.e.r. Experiments at Pt provide the opportunity of direct electrochemical study of the competitive adsorption of As species *vis-à-vis* chemisorption of H, the intermediate in the h.e.r. The As arises from the HF used in the process and originates from the fluorapatite minerals from which HF is made. The presence of the As in the HF leads to poisoning of the h.e.r. at the cell cathodes, with undesirable increase of overvoltage as well as serious long term degradation of the mild steel cathodes that are used, on account of production of hydrogen which permeates into the metal leading to embrittlement and spalling.

One of the major matters of fundamental interest [1, 4–6] in the effects of catalyst poisons on the h.e.r. is their influence on the coverage by the overpotential-deposited (o.p.d.) H intermediate and the related, usually inhibitive, effects on the kinetics of the h.e.r. Changes of the o.p.d. H coverage can only be determined indirectly by means of non-steady-state experiments, for example, a.c. impedance or analysis of potential–relaxation transients, as in the present work.

In this work, poisoning effects arising from As species derived from arsenious oxide (As_2O_3), AsF_3 and AsF_5 added into the KF · 2HF melt used in electrolytic fluorine production, on the adsorption behaviour of H and the polarization in the h.e.r. at mild steel cathodes and at Pt as a model electrocatalytic surface were quantitatively studied. Elemental As or compounds such as AsH_3 and AsF_3 having lone-pair electrons, are easily combined with empty emergent *d*-orbitals at the surface of transition metals. It is this feature that leads to strong adsorption of As compounds at electrode surfaces and such processes are usually irreversible. The effects of a poison can be characterized by determining the chemisorption energy or the strength of its bonding to surface atoms or, more indirectly, its effects on cathodic hydrogen evolution kinetics and chemisorption of the H intermediate in that process [3]. The occupancy by the poison species of surface sites on the electrode generally diminishes the coverage by the adsorbed H [1, 5] and decreases currents at given potentials in

0021-891X

the h.e.r. [4]. Adsorbed poisons will not only competitively occupy available adsorption sites but can also lead to interaction forces with the H atoms already covering the surface, or statistically co-adsorbed with the poison [3, 4].

According to Schultze and Koppitz [7], when an adsorbate species 'S' comes in close contact with a metal M, a partial transfer of electron charge is possible (depending on the chemical nature of the adsorbent and adsorbate): $M + S \rightarrow M-S^{\delta+} + \delta e^-$ (in M). However, this charge transfer is usually only incomplete, resulting in a partial charge-transfer related to so-called 'electrosorption valency', which depends, amongst other factors [7], on the difference of electronegativities between the metal substrate and the adsorbate.

Although, in most experiments, arsenic was introduced into the melt as As_2O_3, it is probable that the effective poisoning species are As(0) and As(−III), as AsH_3, which arise on account of electrochemical reduction of the initially added As(III). It is known that poisoning elements are more strongly chemisorbed when they are in low oxidation states, corresponding to greater donicities or lower electronegativities. In fact, elemental As can be deposited electrolytically as a semimetal in the h.e.r. [8] and we have also demonstrated in the present work that AsH_3 is detectable in the evolved hydrogen gas in the $KF \cdot 2HF$ melt initially containing an As(III) species.

The kinetics of the h.e.r. are sensitively influenced by adsorption of catalyst poisons such as As or thiourea [3], which decrease the coverage of the o.p.d. H intermediate. It is also known [9–11] that adsorption of catalyst poisons promotes the cathodic sorption of H into host transition-metal lattices such as Fe, Ni, Ti and Pd. The sorption involves diminished adsorption of H but a facilitated transfer to a subsurface state [5, 11], followed by diffusion into the bulk.

When trace amounts of As_2O_3 or AsF_3 are added into the electrolyte, significant changes arise in the kinetic behaviour of the h.e.r. which are manifested already at quite low concentrations of As species in the potential–relaxation behaviour and the steady-state kinetics of the process. The rate equation for steps in the h.e.r. should then be modified by involvement of the coverage, θ_P, of the poison and an interaction 'g' factor [1, 12] in the form of a Frumkin-type isotherm [13], which enable the potential–relaxation transient behaviour for such conditions to be interpreted. Complementary investigations of poison effects on the u.p.d. H at the Pt model electrode surfaces are also useful and were performed by means of cyclic voltammetry.

2. Experimental details

2.1. *General procedures*

The effects of trace amounts of the As poison species, added into the $KF \cdot 2HF$ melt as As_2O_3 on the state of adsorption of o.p.d. H species in the h.e.r. at Pt and mild steel electrodes were investigated by means of the potential–relaxation method [14, 16] and associated numerical simulations by means of the kinetic 'rate equations' approach [3, 14]. Complementary cyclic voltammetry measurements on the model Pt surface were conducted to evaluate effects of the As poison on the u.p.d. H (cf. [1, 3, 6] for aqueous solution studies). Steady-state Tafel polarization measurements were conducted potentiostatically by means of a computer-controlled system, each potential/current–density point being recorded after 4 s.

In most experiments, the initially added poison species was As_2O_3 of analytical grade obtained from Aldrich. Gravimetrically measured amounts of As_2O_3 powder were introduced into the melt where they became easily dissolved. Concentrations are expressed as atomic percent (at %) with respect to the melt moles. In other experiments, the effects of As as AsF_3 and AsF_5 were compared. In the case of AsF_5 (a gas at 85 °C), the gas was flowed into the melt for 10 min. AsF_3 was injected into the bottom of the melt from a calibrated syringe connected to a Teflon spaghetti tube.

2.2. *Cell and electrodes*

A transparent cell, made of acrylic polymer, which is resistant to attack in the $KF \cdot 2HF$ medium, was used for containing the $KF \cdot 2HF$ melt at the 85 °C experimental temperature. The latter was maintained by a heated air-thermostat oven. Purging by nitrogen or hydrogen gases was not necessary since it was found that the solubility of oxygen in the melt was very small and, in addition, any such bubbling would have caused disturbance and enhancement of evaporation of HF.

A Fe/FeF_2 electrode, made of pure iron wire that had been dipped in the melt for a long time, producing a film of FeF_2, was used as a reference. The iron wire was then sealed into a Teflon tube with its tip situated close to the working electrode, acting as a Luggin probe. All potentials referred to in this paper were recorded with respect to a Fe/FeF_2 reference electrode immersed in the melt. A glassy, carbon counter electrode was mounted in a separate compartment of the cell where fluorine gas was evolved.

The bright platinum working electrode was made from 99.99% pure Pt wire supplied by Johnson Matthey. The mild-steel electrodes, obtained from Cameco Corporation, Saskatoon, were of the same material as that employed as cathodes in the industrial fluorine-production cell. Their surfaces were polished by 800, 1200, 2400 sandpapers sequentially to provide reproducible working surfaces.

2.3. *Open-circuit potential–relaxation transients*

The open-circuit potential–relaxation transients were recorded as described previously [1, 3], following interruption of previously recorded currents by

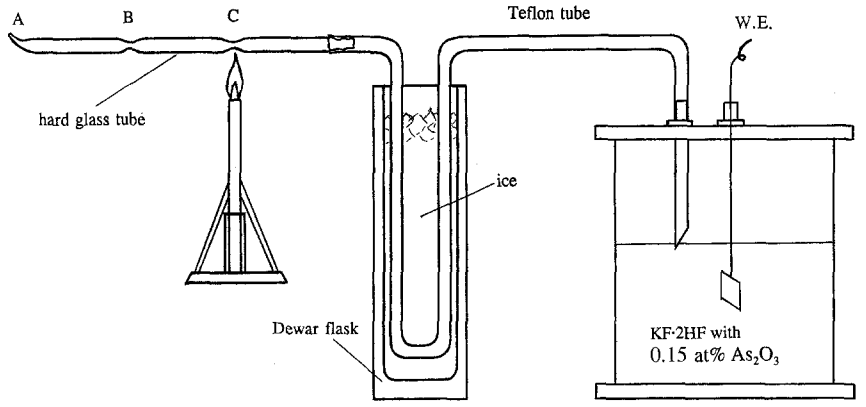

Fig. 1. The apparatus for testing for generation of small amounts of AsH_3 in the electrolytically generated hydrogen at a mild steel cathode by means of Marsh's test.

means of a vacuum mercury switch, which gave clear interruptions of current within a very short time (~1 μs). The Pt electrodes were first depoisoned by polarizing at +1.6 V, where surface poisons were oxidized and dissolved. Before the current interruption, the surfaces were repoisoned at selected cathodic potentials for 5 s in each experiment. The potential against time relaxation transients were recorded digitally using two Nicolet oscilloscopes in tandem, covering a total of six or seven decades of time range, starting in the microsecond region. It is very important that 'full-range' potential–relaxation transients be recorded in order to make kinetic simulations of the experimental data, that is, for transients in which the potential relaxes down to, or near, the reversible potential. Control experiments in the absence of As poison were performed for appropriate initial current-densities. the *iR* drops have already been corrected for the transient curves in the Figures.

The full potential–relaxation behaviour [3, 14] is determined by the kinetic equations for steps in the h.e.r. which involve the rate of electron consumption, or faradaic current, and the rate of production of MH, the H intermediate adsorbed at M [14, 16]. The two resulting kinetic relations are stiff ordinary differential equations, which can be solved numerically. The simulation of the experimental transients was realized in this way using a nonlinear least-squares (NLSQ) procedure, as used in previous work [3].

2.4. *Cyclic voltammetry*

Cyclic voltammograms (CV) were also recorded at the Pt electrodes over the u.p.d. H potential range, using an HB-104 HD function generator and an HA-301 HD potentiostat. The signal outputs were recorded by one of the Nicolet oscilloscopes, using a low-frequency filter to eliminate electronic noise which arose under some conditions.

2.5. *Contact angle measurements*

It has been found in previous related work [15] that in the KF · 2HF melt detachment of electrolytically generated bubbles of hydrogen was sluggish owing to contact angle and surface tension effects. *In situ* contact angle measurements were carried out in the melt using the Rame-Hart Inc. optical-imaging contact angle goniometer (model 100-00). During the contact angle measurements, the hydrogen bubbles were maintained on the electrode surface until no change was observed. Comparative determinations of bubble contact angles at poisoned and unpoisoned mild steel surfaces were made in the KF · 2HF melt. The solid/liquid/gas interface was photographed and the contact angle measured from the image picture.

2.6. *Formation and detection of AsH_3*

AsH_3 can be formed from As-containing electrolytes by cathodic reduction of As(III); its detection is based upon the fact that arsine, when conducted through a heated glass tube, becomes decomposed into hydrogen and a visible film of the metalloidal element As (Marsh's test [17]) which is deposited as a brownish-black 'mirror' just before the heated part of the tube (the decomposition temperature of AsH_3 is about 300 °C).

A special test system (Fig. 1) was constructed for determining whether small amounts of AsH_3, electrogenerated, could be detected in the hydrogen gas evolved at the mild steel cathodes. In the electrolytic cell, the ambient gas contains H_2, HF and AsH_3, and they have different densities ($d(H_2) = 0.0899$ g dm^{-3}; $d(HF) = 0.991$ g dm^{-3}; $d(AsH_3) = 2.695$ g dm^{-3}). The AsH_3 gas is the 'heaviest' one (most dense), so the gas-collecting (sampling) tube must be put at a low position, just above the melt surface in the cell. This gas mixture was generated by cathodically polarizing the mild steel electrode galvanostatically at -40 mA cm^{-2} in the KF · 2HF melt in the presence of added As(III) for 3 h. The HF, which is also unavoidably collected in the gas can be condensed after passing through a trap at 0 °C (the boiling point of HF is 19.5 °C, that of AsH_3 is −55 °C). The remaining $H_2 + AsH_3$ gas mixture was then passed into a heated glass tube for application of Marsh's test.

2.7. *The KF·2HF melt*

To prepare clean KF·2HF melts, the purest commercially available KF·HF (99+%, Johnson Matthey) and 99.9% HF (Matheson Gas Products, Canada) were mixed quantitatively in a high-density polyethylene bottle, in which the exothermal reaction, $KF \cdot HF + HF \rightarrow KF \cdot 2HF$, took place.

The phase diagram of the KF/HF system [2, 18] indicates that its melting point sharply increases below the composition KF·1.87 HF. The operating temperature was around 85 °C in the experiments, higher than the melting point (71.7 °C) of the KF·2HF [19]. Evaporation or electrochemical consumption of HF during polarization experiments causes a small but significant change of composition and correspondingly of the melting point of the mixture, as was found in our previous experiments [2]; this leads to a major contribution to the so-called 'hyperpolarization effect' [2] in the cathode reaction due to formation of a thin, poorly conducting film of solid electrolyte at the cathode interface. However, by supplying calculated amounts of KF·3HF melt into the consumed KF·2HF melt, the change of composition can be compensated and the 'hyperpolarization effect' eliminated [2].

The conductivity of the melt arises in part from proton hopping, like the proton conductance mechanism in acid or alkaline aqueous solutions [20], viz.

$$F{-}H + F^- \longrightarrow F^- + H{-}F \longrightarrow F{-}H + F^- \longrightarrow F^- + H{-}F \ldots \text{etc.} \quad (1)$$

Such a process can continue in the solid state as is known, for example, for proton transport in ice [21] and in solid $HClO_4 \cdot 5H_2O$. This provides some residual solid-state conductivity.

The 'acidity' of the KF·2HF melt may be considered in relation to analogy with the aqueous system. Like H_2O, autoprotolysis in HF ($3HF \rightleftharpoons H_2F^+ + FHF^-$) is weak, analogous to that in H_2O ($K_w = 10^{-14}$). The pH of the system is represented by $-\log[H_2F^+]$. Corresponding to KOH in the aqueo-system, KF in HF is therefore an 'alkaline' solution, that is, the KF·2HF solvate is to be regarded as an 'alkaline system' in the HF solvent, like $KOH \cdot 2H_2O$ in water (cf. [15]).

3. Results and discussion

Examination of the kinetic behaviour of the cathodic process at Pt and steel electrodes in the KF·2HF melt constitutes a new direction of study of the h.e.r., conducted for the first time in the present work. In the presence of As_2O_3, and also of AsF_3, the kinetic behaviour of the h.e.r. as well as the u.p.d. H adsorption, are influenced mainly through competitive adsorption of an arsenic poison species at the active sites on the metal. Lateral interactions amongst the adsorbed poison species and H can also cause change of H coverage at a given η and a modification of the surface electronic structure of the electrocatalyst, and hence modify the catalytic behaviour of the metal electrode surface [11].

3.1. *Cyclic voltammetry at Pt in As_2O_3-poisoned KF·2HF melt*

The poisoning effect of As_2O_3 on the adsorption behaviour of the (u.p.d.) H at Pt was studied by means of cyclic voltammetry (CV) at $100\,mV\,s^{-1}$. Fig. 2 shows the CV plots for bright Pt in the KF·2HF melt at 85 °C with the addition of 7×10^{-4} at % of As_2O_3. Over the potential range 0.2 to 0.5 V (vs Fe/FeF_2), where the u.p.d. monolayer of H is formed, the peaks and the charges for the u.p.d. H in the presence of poison are diminished in comparison with those for the clean melt. The adsorbed As poison species, as may be expected (cf. Frumkin and Slygin in [24]), competitively occupy the active sites which would otherwise be taken by the u.p.d. H over this potential region. It is interesting to see that an oxidation peak at about 1.0 V and a reduction peak at about 0.7 V can also be clearly identified. These seem to be due to oxidation and reduction reactions of the electrosorbed arsenic species. Further cycling to more positive potentials leads to formation of a surface fluoride at the Pt electrode, and As(V) (as AsF_6^-) may then also be produced and became dissolved into the electrolyte.

Comparison of the voltammograms at Pt for potentials taken up to 1.75 V vs Fe/FeF_2 in the absence (dotted curve in Fig. 2) and in the presence of As (solid line curve in Fig. 2) indicates some significant remaining diminution of the anodic currents and of the extent of fluoride film formation (as indicated by the diminished area under the surface-fluoride reduction peak at 1.02 V). This suggests that over the timescale and potential range of these voltammograms the arsenic species are only incompletely oxidatively desorbed. This receives confirmation from the fact that the returning cathodic current profile from potential-sweep reversal at 1.75 V reveals some appreciable residual blocking of electrosorbed H (by about 30%) over the potential range 0.5 to 0.22 V vs Fe/FeF_2. Probably the electrosorbed As species [As(0) and AsH_3] require several anodic/cathodic cycles for its removal or a more positive potential reversal limit in the voltammogram.

When the upper limit of cycling is decreased to 1.1 V or 0.8 V, the u.p.d. H peaks are further suppressed. This is because the arsenic poison then remains on the surface, occupying adsorption sites at Pt, and causes the u.p.d. H adsorption to diminish under conditions where the arsenic species is not, or not fully removed by oxidation at the higher potentials.

3.2. *Treatment of potential–relaxation transients recorded for the HER*

3.2.1. Theoretical basis. Elsewhere [1, 3], we have

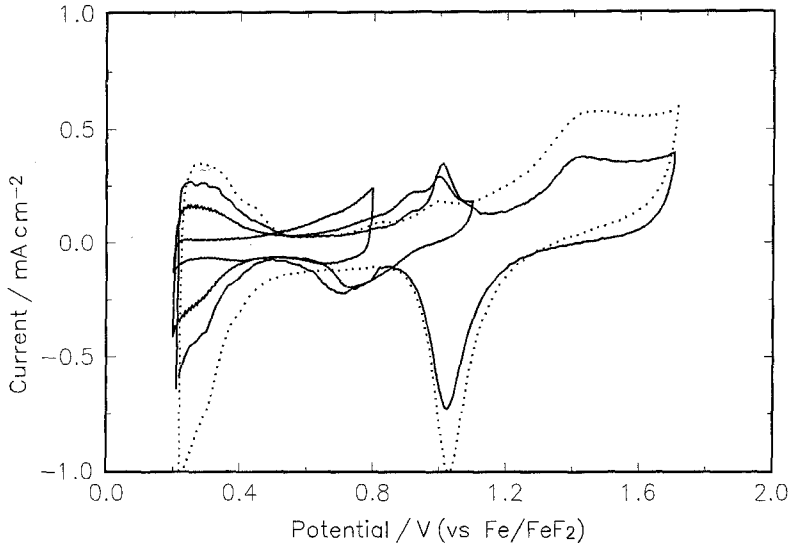

Fig. 2. Cyclic voltammograms (CV) at Pt in the KF · 2HF melt, at a sweep rate of 100 mV s^{-1}. Dotted line is CV in the clean melt; solid lines are CVs in the presence of 7×10^{-4} at % As_2O_3 in melt, for different positive limit potentials. Key: (· · ·) clean; (——) poisoned.

shown that recording of potential–relaxation transients, following interruption of hydrogen gas evolution currents, can provide useful information on the role and extent of adsorption of H in the h.e.r. The required theoretical procedure, summarized below, was applied to comparative studies on the As-poisoned electrode surfaces by means of computer simulation calculations.

The h.e.r. in the HF melt can proceed via three steps, analogous to those in water, viz. electrosorption of H, followed by the 'atom-ion' electrodesorption of H and/or by desorptive recombination, as follows, including respective back-reactions:

$$\text{Step 1} \quad M(e) + HF \underset{k_{-1}}{\overset{k_1}{\rightleftharpoons}} MH_{ads} + F^- \tag{2a}$$

Step 2

$$MH_{ads} + M(e) + HF \underset{k_{-2}}{\overset{k_2}{\rightleftharpoons}} H_2 + F^- + 2M \tag{2b}$$

or

$$\text{Step 3} \quad 2MH_{ads} \underset{k_{-3}}{\overset{k_3}{\rightleftharpoons}} H_2 + 2M \tag{2c}$$

For the idealized and simple case, where the metal surface is covered only by adsorbed H, the h.e.r. behaviour is usually described in terms of a Langmuir isotherm for adsorption of the H intermediate, although such an isotherm does not strictly apply to u.p.d. H at Pt. In the present study, with the involvement of poison adsorption, surface heterogeneity and lateral-interaction effects should also be considered. It is assumed as a reasonable approximation (cf. [22]) that the rate constants decrease exponentially with increasing coverage of adsorbed species when the lateral interaction effects are significant.

The calculation of the rates of the electrochemical processes involving poisons was made by modifying the Langmuir isotherm equations, considering both the coverage of poison, θ_P, and the lateral interaction factor, g [1, 22]. For the steps of the h.e.r. in Equations 2, the separate rates of each of the individual forward and backward steps of the reaction are represented by the following equations:

$$v_{1,f} = k_1(1 - \theta_H - \theta_P)\exp[-\beta g(\theta_H + \theta_P)] \times \exp[-F\eta/2RT]$$
$$= k'_1(1 - \theta_H - \theta_P)\exp[-F\eta/2RT] \tag{3a}$$

$$v_{1,b} = k_{-1}\theta_H \exp[(1-\beta)g(\theta_H + \theta_P)]\exp[F\eta/2RT]$$
$$= k'_{-1}\theta_H \exp[F\eta/2RT] \tag{3b}$$

$$v_{2,f} = k_2\theta_H \exp[\beta g(\theta_H + \theta_P)]\exp[-F\eta/2RT]$$
$$= k'_2\theta_H \exp[-F\eta/2RT] \tag{3c}$$

$$v_{2,b} = k_{-2}(1 - \theta_H - \theta_P)\exp[-(1-\beta)g(\theta_H + \theta_P)] \times \exp[F\eta/2RT]$$
$$= k'_{-2}(1 - \theta_H - \theta_P)\exp[F\eta/2RT] \tag{3d}$$

$$v_{3,f} = k_3\theta_H^2 \exp[2\beta g(\theta_H + \theta_P)]$$
$$= k'_3\theta_H^2 \tag{3e}$$

$$v_{3,b} = k_{-3}(1 - \theta_H - \theta_P)^2 \exp[-2(1-\beta)g(\theta_H + \theta_P)]$$
$$= k'_{-3}(1 - \theta_H - \theta_P)^2 \tag{3f}$$

In Equations 3(a)–(f) the surface concentrations of the reagent are included in the rate constants. θ_H is the fractional coverage by H and θ_P that by poison, P; g is a two-dimensional lateral interaction factor [22]. Here η is taken as negative for a cathodic process. The exponential term involving the $\beta g\theta$ factor in the rate equations corresponds to a change of activation energy with coverage communally by H and P due to interactions. For $g > 0$ the interaction is repulsive amongst the adsorbed atoms. v_f and v_b represent forward and backward rates of each reaction step, and the net rate $v = v_f - v_b$, applies to each step. k' values are quantities involving an exponential term in which β, g, θ_H and θ_P factors are included.

The theoretical basis of the simulation treatment of the potential–relaxation and H adsorption behaviour

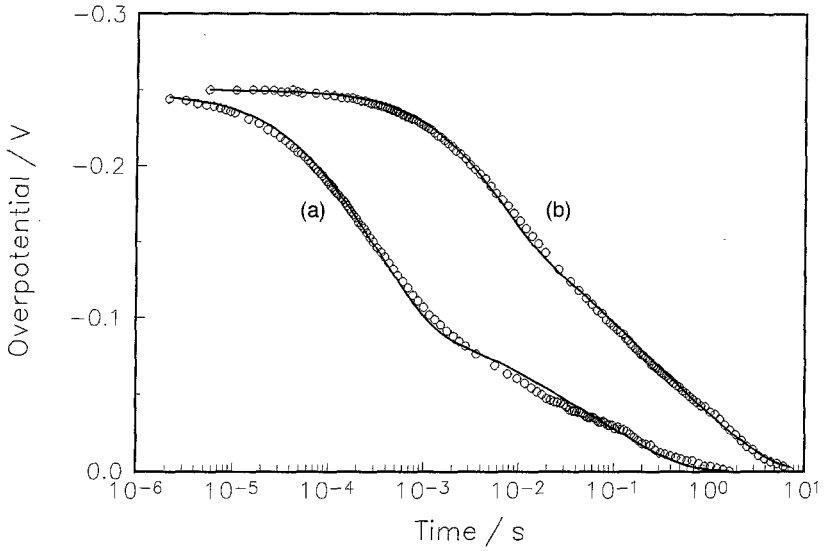

Fig. 3. Potential–relaxation transients at Pt in the KF · 2HF melt. The points represent the experimental data and the solid line the curve for best fit of the results by kinetic simulation. Curve (a) is the transient in the clean melt; curve (b) is that in the presence of 7×10^{-4} at % As_2O_3 in the melt.

in the h.e.r. has been presented and discussed previously [1, 14]. Nonlinear least-square fitting of the experimental data to the kinetic functions yields values of the kinetic parameters for the system under study, including the rate constants and the coverages by H and poison, P. Since the poison species are usually irreversibly adsorbed on the surface, θ_P is considered unchanged in each simulation of potential–relaxation. This calculated θ_P has the value for adsorption at the electrode surface at the moment of current interruption after 5 s polarization at a designated overpotential.

3.2.2. Potential–relaxation transients for the h.e.r. at Pt in As_2O_3-poisoned KF · 2HF melt. Figure 3 shows the potential–relaxation transients for the h.e.r. at the Pt electrode after introduction of 7×10^{-4} at % of As_2O_3 (curve (b)) in the KF · 2HF melt in comparison with the behaviour in clean As-free melt (curve (a)). The arrest in curve (a) over the 10^{-3} to 1 s range is due to the electrochemical desorption of the previously discharged H intermediate in the transient process [1, 14]. The transient in the presence of the poison shifts to a longer time domain (curve (b)) than that for the clean melt (curve (a)), and the arrest disappears on curve (b), due to the diminution of H adsorption and consequent decrease of its pseudocapacitance [1, 14] through site-occupancy competition by the arsenic species.

Quantitatively, kinetic parameters for the h.e.r. at the unpoisoned and poisoned Pt electrodes were derived from kinetic simulations of curves (a) and (b), as recorded in Table 1. Curve (a) for the unpoisoned melt was simulated, taking $\theta_P = 0$ and $g = 0$, as for the cases of clean solutions [14, 23] studied previously. Apparently, as might be intuitively expected, the k values for the poisoned melt are much smaller than those without poison, corresponding to inhibition of the h.e.r. by the poison adsorption. Other quantities or parameters, e.g. g and θ_P, were also evaluated, as listed in Table 1.

The relations of θ_H and C_ϕ to η for unpoisoned and poisoned surfaces are plotted in Fig. 4a and 4b, respectively. In Fig. 4(a), corresponding to curve (a) of Fig. 3 for the unpoisoned melt, the fractional coverage, θ_H by H, rapidly approaches to 1 at overpotentials more than −0.1 V, which means full o.p.d. H coverage tends to be attained at high overpotentials. The H pseudocapacitance, C_ϕ, is on the scale of mF cm^{-2} (cf. [22]). The 'peak' position of C_ϕ shifts to lower overpotentials (approach to the equilibrium potential region), which indicates diminution of the k_1/k_{-1} ratio, that is, a greater relative kinetic participation of the back reaction in step 1, as discussed in [3], for As poisoning effects in aqueous solution at Pt.

In Fig. 4(b) for the poisoned surface corresponding to curve (b) of Fig. 3, θ_H reaches 0.46 at −0.4 V, while the calculated $\theta_P = 0.53$. The derived θ-values are accurate to about 7% bearing in mind the data-fitting processes that are involved. The H pseudocapacitance, C_ϕ, is also diminished due to the restriction of coverage by o.p.d. H caused by the competition of adsorbed poison species. The variation of θ_H with potential becomes small which is attributed to the effect of increase of the value of k_3 in the reaction.

Table 1. Comparison of parameters for simulation of the kinetics of the h.e.r. at Pt in unpoisoned and 7×10^{-4} at % As_2O_3-poisoned KF · 2HF melt

KF · 2HF melt	*Unpoisoned*	*As_2O_3 poisoned*
k_1/mol cm^{-2} s^{-1}	2.0×10^{-7}	1.6×10^{-10}
k_{-1}/mol cm^{-2} s^{-1}	3.0×10^{-8}	2.1×10^{-10}
k_2/mol cm^{-2} s^{-1}	3.8×10^{-10}	1.0×10^{-15}
k_3/mol cm^{-2} s^{-1}	3.5×10^{-14}	2.3×10^{-11}
C_{dl}/μF cm^{-2}	8.94	6.49
q_1/μC cm^{-2}	115	8.5
g	(0)	3.3
θ_P	(0)	0.53

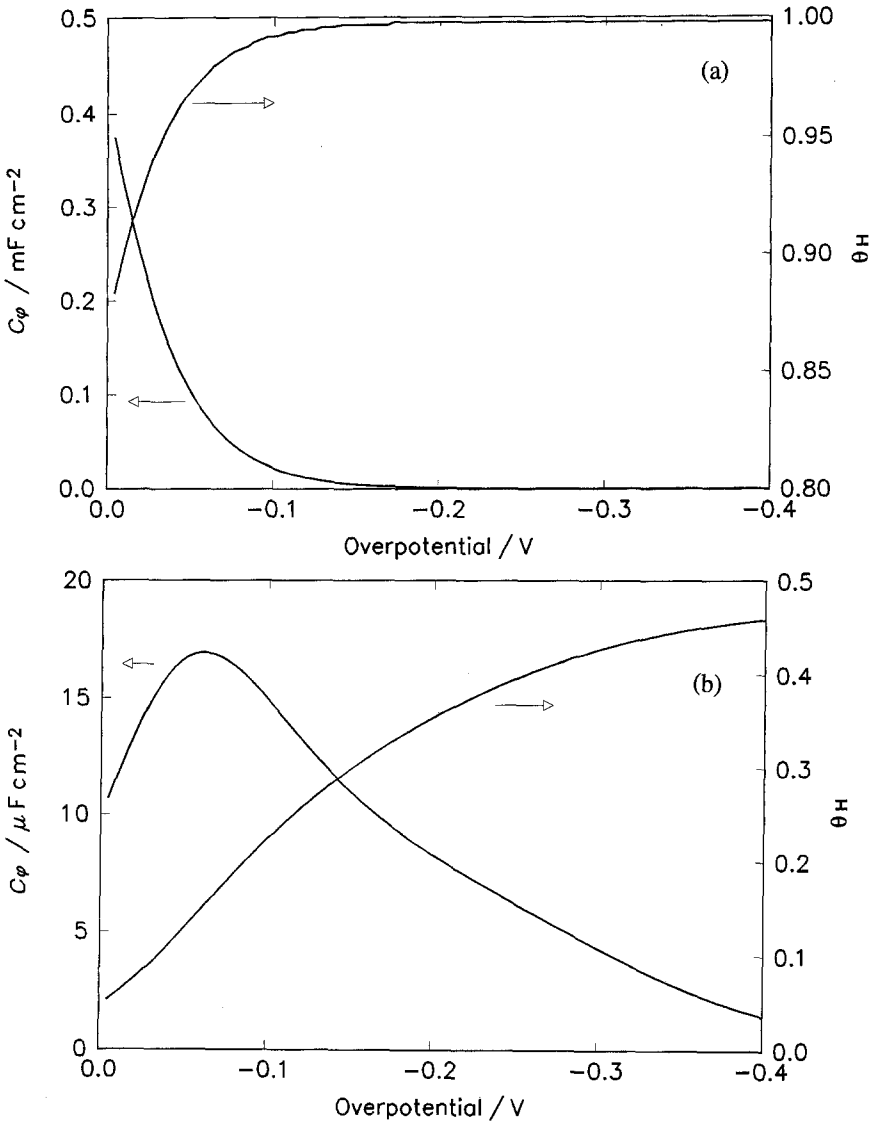

Fig. 4. Relations of pseudocapacitance, C_ϕ, and coverage by H, θ_H, against overpotential, calculated by kinetic simulation of the transients at Pt; (a) in the clean melt corresponding to curve (a) in Fig. 3; (b) with 7×10^{-4} at % As_2O_3-added melt, corresponding to curve (b) in Fig. 3.

Thus, the recombination step interestingly becomes *more* significant in the presence of poison, since physically, poisons adsorb on the surface sites and prevent H from further adsorption; this, in fact, promotes H desorption through repulsive interaction in step 3, although the probability of occupation of nearest neighbour sites by H will tend to be diminished.

3.2.3. Potential–relaxation transients for the h.e.r. at mild-steel in As_2O_3-poisoned KF·2HF melt. Comparative experiments were also carried out at mild-steel electrodes as used in fluorine-production cells. Figure 5 shows the potential-relaxation transients at unpoisoned (curve (a)) and poisoned (curve (b)) mild steel cathodes in the KF·2HF melt. Points represent the experimental data and solid lines the computer simulated results. The arrest in curve (a) in Fig. 5 is less pronounced than that in curve (a) of Fig. 3, which means the extent of adsorption by o.p.d. H at mild-steel is less significant than at Pt in the clean melt. In the presence of As_2O_3, the transient (curve (b)) extends over a longer time domain and the arrest disappears, as similarly observed in Fig. 3.

In the case of the mild-steel electrodes, the possibility of the corrosion reaction $2HF + Fe \rightarrow Fe^{2+} + H_2 + 2F^-$ interfering with the hydrogen overpotential relaxation transients (Fig. 5) has to be taken into account.

In previous work the experimentally measured thermodynamic potential of the Fe/FeF_2 electrode vs the hydrogen electrode potential in the melt was found to be −0.185 V which is similar to the value that could be deduced approximately in Fig. 2 from the least positive sweep reversal potential in the u.p.d. H region of the voltammograms. The corrosion mixed potential is at +0.012 V positive to the Fe/FeF_2 reversible electrode potential. Hence interference with the declining potential in the transients, taken from appreciable cathodic overpotentials in the hydrogen evolution reaction (Fig. 5), will arise only near the corrosion potential (+0.012 V vs Fe/FeF_2); over most of the potential range of the transients, the steel electrode will, in fact, be under a condition of cathodic protection. Of course, for the transients taken at Pt (Fig. 3), the above problem does not arise.

From the kinetic simulation of the two curves,

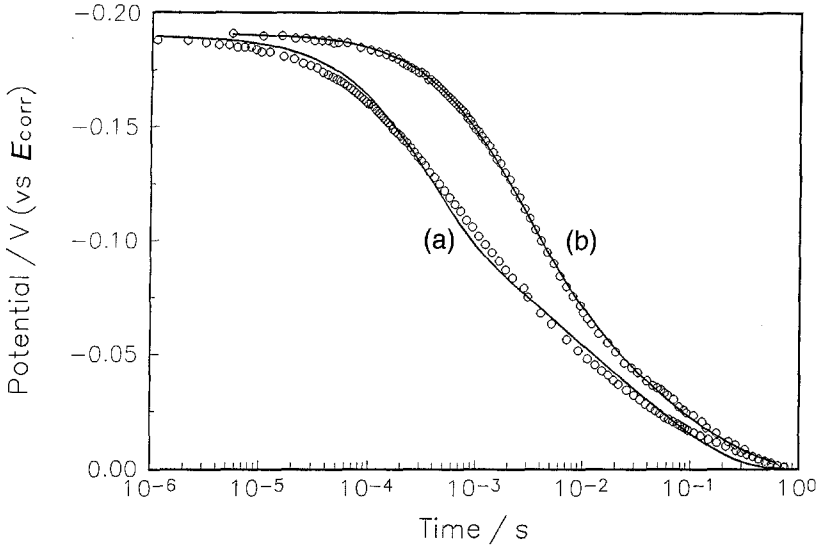

Fig. 5. Potential–relaxation transients at the mild steel electrode in the KF · 2HF melt. Curve (a) is the transient in the clean melt; curve (b) that in the presence of 7×10^{-4} at % As_2O_3 in the melt.

kinetic parameters were determined as listed in Table 2, which shows that decreased rate constants arise for the poisoned mild steel, and values of the parameters $g = 5.2$ and $\theta_P = 0.71$ are also obtained. Again the value of k_3 increases for the poisoned electrode, indicating an increasing significance of the recombination reaction in the two alternative H desorption steps, 2b and 2c.

The relations of θ_H and C_ϕ to η at the mild steel electrodes are similar to those shown in Fig. 4 for Pt electrodes, except the magnitudes of θ_H and C_ϕ are smaller in this case, due to less H adsorption and larger coverage of adsorbed poison at the mild steel surfaces.

3.3. *Polarization behaviour and the contact angle of hydrogen bubbles at mild-steel electrodes*

The present results show that adding As_2O_3 to a pure KF · 2HF melt has a strong effect, like that at Pt, on the cathodic polarization behaviour of mild steel electrodes. It is also found that hydrogen bubble detachment becomes very sluggish because of an increase of interfacial contact angle.

Figure 6 shows the Tafel behaviour at a typical mild steel electrode before and after addition of 2.5×10^{-3} at % As_2O_3. It is clearly seen that the cathodic currents become much smaller in the presence of As species; the poison diminishes the electrocatalytic activity of the mild steel cathode. It is seen in Fig. 6 that current 'jumps' arise; this is because large hydrogen bubbles become sluggishly and irregularly detached from the electrode surface, a phenomenon characteristic of the KF · 2HF melt [2, 15].

Table 2. Comparison of parameters for simulation of the kinetics of the h.e.r. at the mild steel electrode in unpoisoned and 7×10^{-4} at % As_2O_3-poisoned KF · 2HF melt

KF · 2HF melt	*Unpoisoned*	*As_2O_3 poisoned*
k_1/mol cm^{-2} s^{-1}	1.2×10^{-7}	3.0×10^{-9}
k_{-1}/mol cm^{-2} s^{-1}	1.7×10^{-8}	1.2×10^{-8}
k_2/mol cm^{-2} s^{-1}	1.9×10^{-10}	4.4×10^{-14}
k_3/mol cm^{-2} s^{-1}	2.2×10^{-13}	8.0×10^{-9}
C_{dl}/μF cm^{-2}	4.08	5.28
q_1/μC cm^{-2}	65	3.4
g	(0)	5.2
θ_P	(0)	0.71

To examine the above phenomenon more quantitatively, the hydrogen bubble/electrode contact angles in the melt, without and with addition of As_2O_3, were measured as shown in Fig. 7(a) and (b). The bubbles formed at the mild steel electrode in the melt in the absence of As species were spherical in shape (circular image), the measured contact angle being $46° \pm 3°$. However, in the presence of As, the hydrogen bubbles attached tightly to the mild-steel surface and tended to grow larger in size than detaching; it had become more difficult for the mild steel to be wetted by the melt (electrolyte). The contact angle was then $108° \pm 5°$, determined by drawing a tangent line at the contact point of the hydrogen bubble/KF · 2HF/mild steel interface. The difference in the way the hydrogen bubbles reside at the steel surface in the presence and absence of poison is clearly seen in Fig. 7(a) and (b).

3.4. *Polarization behaviour of steel cathodes in KF · 2HF melt in the presence of AsF_3 and AsF_5*

Studies of cathodic polarization at the mild steel cathodes were also made in the presence of AsF_3 or AsF_5 as the initial poisoning species. These are the compounds known to be present in the commercially used HF feed from some sources. Figure 8 shows a series of Tafel polarization plots for the h.e.r. at a mild steel cathode taken after three extended periods of time following addition of AsF_5 to the melt. In the presence of AsF_5 which, in the melt, is predominantly in the form of the AsF_6^- complex anion, the poisoning effects arise much more slowly than when

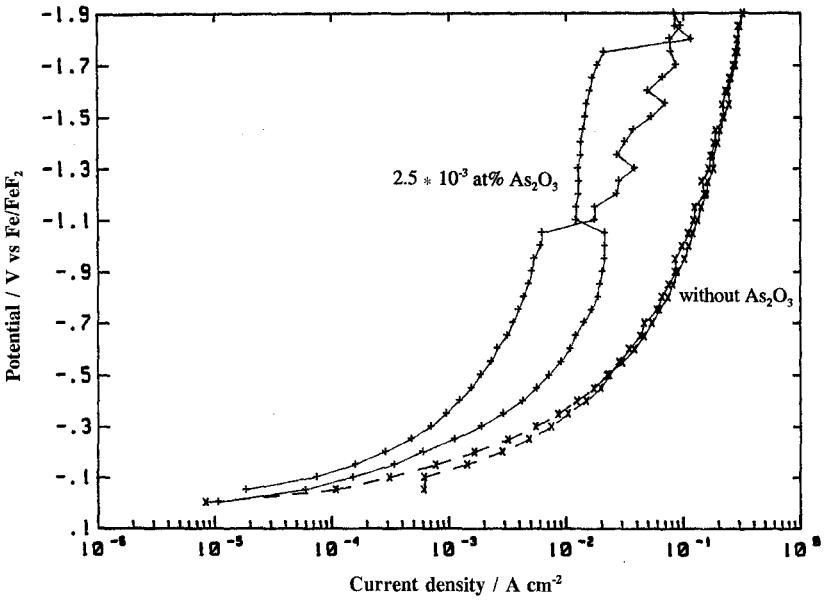

Fig. 6. The polarization behaviour of a typical mild steel electrode in the KF · 2HF melt. (×) points represent the Tafel data for the melt free from As species; (+) points represent data for the melt in the presence of 2.5×10^{-3} at % As_2O_3.

As is initially present as As_2O_3 (Fig. 6) or AsF_3 (Fig. 9(a) and (b)). This, we believe, is due to the stability of As(v) species, especially as AsF_6^-, which have no donor electron pair available on As, so that the poisoning arises only after slow reduction of As(V) to As(III) species; or eventually to As(0) or As(−III), as AsH_3. Similar behaviour arises if the As is added as As_2O_5; then again only slow poisoning arises.

Figure 9(a) and (b) show comparatively the time effects of poisoning in the presence of AsF_3 and AsF_5 on the cathodic hydrogen evolution currents at three or four potential values. It is clear that the effect of added AsF_5 (Fig. 9(b)) is much slower than that of AsF_3 (Fig. 9(a)). Such results suggest that slow electrolytic reduction of As(V) is required before chemisorption of an As species, having a lone pair of electrons, can take place.

3.5. *Detection of arsine at mild-steel cathodes in the KF · 2HF melt in the presence of As_2O_3*

It is known [4, 8] that the following reaction can take place on a cathode surface when the concentration of arsenic species is sufficiently high or polarization duration is long, giving rise to a visible thin deposit of elemental As:

$$As^{3+} \text{ (from added } As_2O_3) + 3e^- + M \longrightarrow M/As^0 \quad (4a)$$

which is then followed by reduction to AsH_3:

$$M/As^0 + 3HF + 3e^- \longrightarrow M + AsH_3 + 3F^- \quad (4b)$$

The cathodically evolved hydrogen bubbles are then generated on an As film electrodeposited on the mild steel substrate surface or that at which AsH_3 is adsorbed or coadsorbed with H. From the contact angle measurements described above, substantial changes of contact angles of hydrogen bubbles at As-covered mild steel electrodes are found and this is the main reason why sluggish detachment of hydrogen bubbles arises at the As-poisoned surfaces. The presence of such recumbent bubbles tends to isolate areas of the cathode surface and lead to an effect on the polarization due to local modification of the current distribution. This accounts for the irregular current jumps referred to above.

As explained in the experimental section, Marsh's test was applied for qualitative detection of small amounts of arsine that could be present in the gases evolved in the cathodic reaction. A mild steel electrode was polarized galvanostatically at −40 mA cm^{-2} in the KF · 2HF melt with 0.15 at % added As_2O_3. The gases evolved from the electrode were collected and passed through the heated glass tube (Fig. 1). After polarizing for 3 h, a brownish-black 'mirror' deposit was found, as illustrated in Fig. 10, characteristic of As generated by thermal decomposition of AsH_3, the basis of Marsh's test.

Further proof of the existence of AsH_3 was provided by observation that the cathode gases, when passed through a silver nitrate solution, caused blackening on account of the following reaction [17]:

$$6AgNO_3 + 3H_2O + AsH_3 \longrightarrow H_3AsO_3 + 6Ag + 6HNO_3 \quad (5)$$

An easily observable black suspension was formed in the silver nitrate, characteristic of the presence of AsH_3; hydrogen gas itself does not cause such a reduction [17]. These two tests provided a clear indication that AsH_3 (or initially As) was electrogenerated in cathodic polarization and also led to change in the contact angles of hydrogen bubbles.

In considering the significance of these results on As deposition and AsH_3 formation, the question arises whether a steady state has been set up between As deposition and the reduction of AsH_3, coupled with the coevolution of molecular hydrogen.

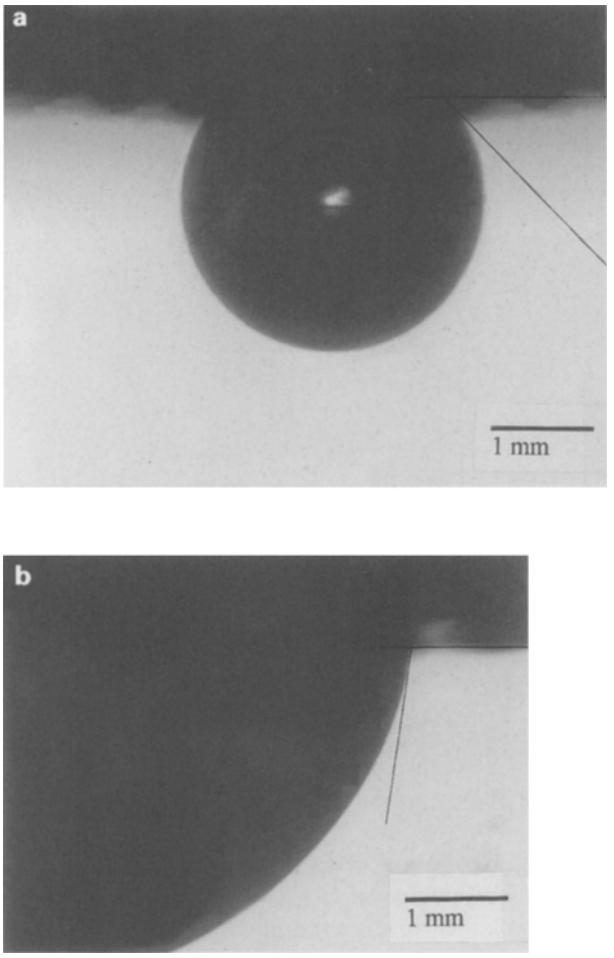

Fig. 7. Photos of magnified hydrogen bubbles formed beneath the mild-steel electrode in the (a) KF·2HF melt; (b) KF·2HF melt with addition of 2.5×10^{-3} at% As_2O_3.

The electrode kinetics of that situation are complex so that attempts at some conclusions would probably be unproductive. Therefore we made the analytical and Marsh test experiments after 3 h period of cathodic electrolysis at the 40 mA cm^{-2} rate, presuming reasonably that such a time would be quite adequate for a steady state to be established. Also, since the As concentration was only 0.15 at %, its reduction would probably be diffusion-controlled anyway so that a steady state would have been set up after a quite short time. Then the steady state coverage by As(0) would be determined by the rate of its electrochemical conversion to AsH_3 (a $3e^-$, $3H^+$ step or chemical steps involving reduction of the As(0) by three coadsorbed H atoms arising from HF discharge) relative to the diffusion-limited rate of elemental As deposition.

3.6. *Ex situ surface analysis of a mild steel electrode polarized in the As_2O_3-poisoned KF·2HF melt*

The mild steel electrode samples which had been polarized in the KF·2HF melt in the presence of 2.5×10^{-3} at% As_2O_3 were examined by means of X-ray photoelectron spectroscopy (XPS) and energy-dispersive X-ray analysis (EDX). The results of such experiments showed that the arsenic is readily observable using the former technique, as shown in Fig. 11, but is not easily detectable using EDX. The sampling depth of XPS is on the order of a few nanometres or less, whereas the sampling depth of EDX is typically 50–500 nm, so relatively, 'As' on the surface, probably as a monolayer of As(0) or AsH_3, is difficult to detect, as might be expected. On the other hand, the XPS surface analysis results show that the As, present in some state as a very thin film on the electrode surface, is detectable. The initially added As (as As_2O_3) becomes present as a thin deposit of As^0 [4, 8] on the electrode surface where it is evidently further reduced to AsH_3 when the electrode is polarized cathodically, and remains, in part, adsorbed, with the remainder co-evolved with the cathodically generated hydrogen. This presumably prevents the As film from being continuously formed and increasing in thickness. The presence of oxygen in the survey spectra of Fig. 11 implies

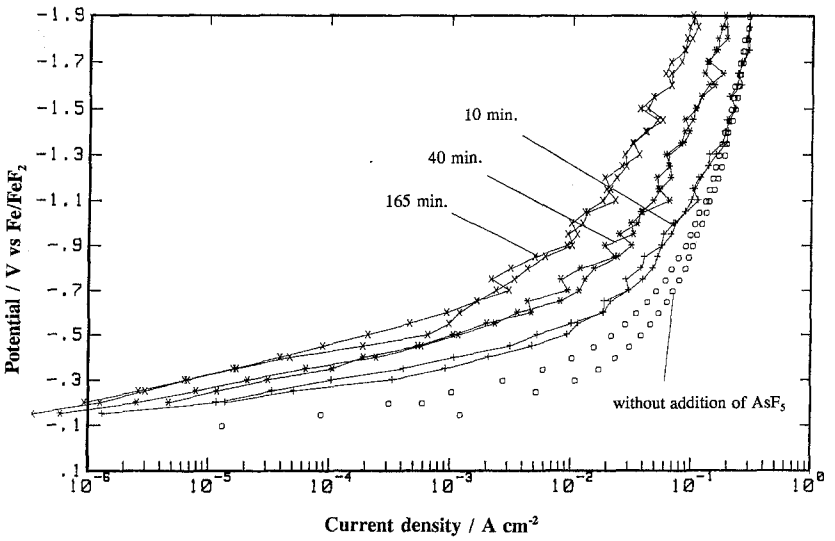

Fig. 8. The polarization behaviour of the mild steel electrode in the KF·2HF melt in the presence of AsF_5 after several periods of time, up to 165 min. Concentration approximately 0.3 at %, or larger. Circle points represent polarization in the absence of AsF_5 in the KF·2HF melt.

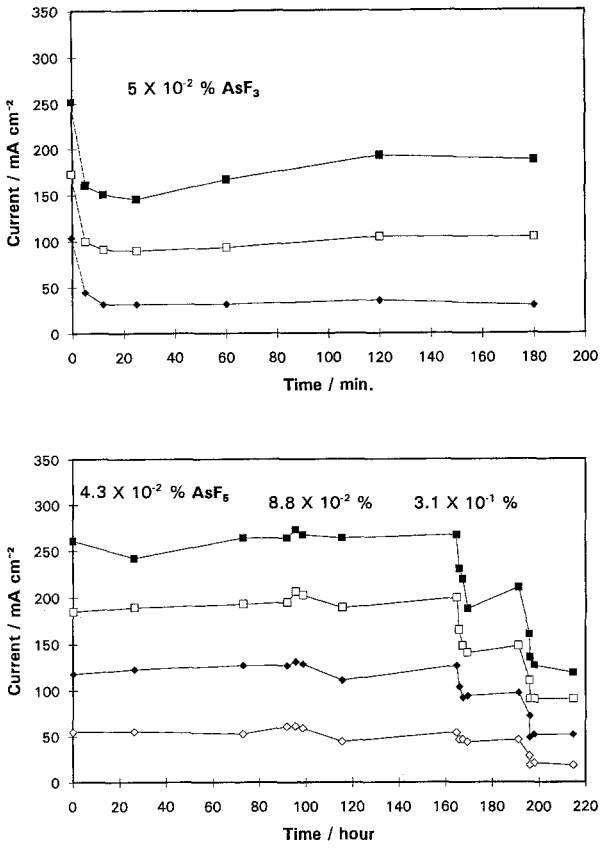

Fig. 9. Comparison of time dependence of cathodic hydrogen evolution currents at several potentials at a mild steel electrode at 85 °C in the KF · 2HF melt in the presence of: (a) AsF_3 (0.05 at %) and (b) AsF_5 (0.043 at %); it was increased to 0.088 at % at 93th hour and then further increased to 0.31 at % at 162th hour.

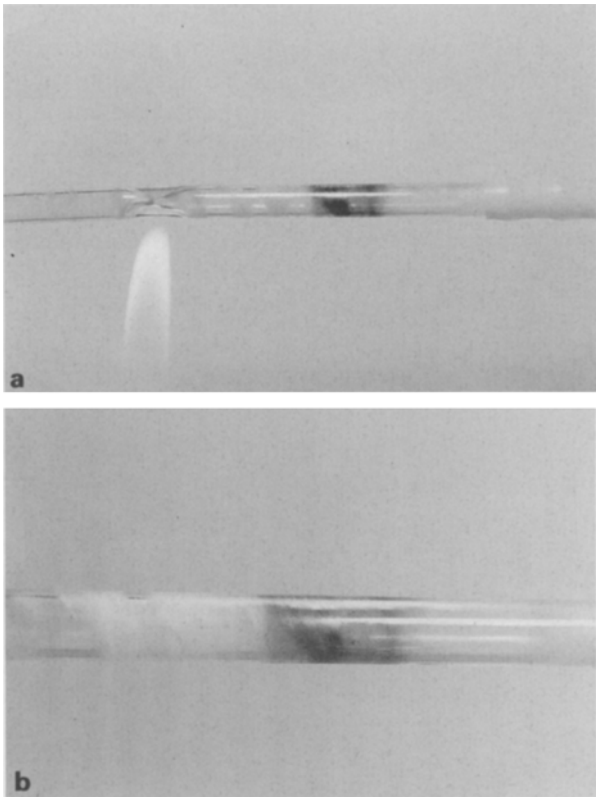

Fig. 10. Pictures of a brownish-black 'mirror' deposit of As on the wall of a heated glass tube due to the presence of AsH_3 in hydrogen cathodically evolved at a mild steel electrode. (Application of Marsh's test).

a possible oxidation reaction of arsenic due to the *ex situ* nature of the XPS experiments.

4. Conclusions

The presence of As_2O_3 species in the KF · 2HF melt leads to catalytic poisoning of the electrode surface and the h.e.r. proceeding thereon. The poison species are electrogenerated and/or strongly adsorbed on the electrode, and competitively diminish the coverage by the adsorbed H intermediate at the electrode surface. The o.p.d. H coverage is thus diminished in the h.e.r., as determined from analysis of potential–relaxation transients for the h.e.r. in the presence and absence of poison. CV measurements at Pt show that the u.p.d. H is also suppressed in the As_2O_3-containing KF · 2HF melt. Quantitative evaluations of the kinetic parameters and surface coverages of H and poison species were made through simulation of the potential–relaxation behaviour, enabling the relations of H coverage and pseudocapacitance to overpotential to be revealed.

Poisoning effects arise slowly in cathodic polarizations when As(v) species (e.g., as AsF_6^-) are present in the melt. The electrolytic reduction of initially added As_2O_3, AsF_3 and AsF_5 leads to As species at lower oxidation states as As(0) or As(−III) which, having lone-pair electrons, chemisorb strongly on the cathode surfaces.

Application of Marsh's test proved the presence of AsH_3 in the evolved hydrogen while a black Ag suspension, detected after passing the evolved gas

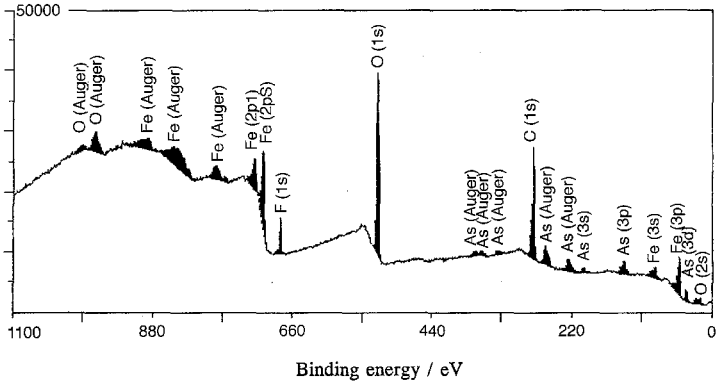

Fig. 11. XPS results for a mild steel electrode after being polarized in the KF · 2HF melt in the presence of 2.5×10^{-3} at % As_2O_3.

into $AgNO_3$ solution, confirmed the presence of AsH_3. The presence of arsenic poison also increased the contact angle of hydrogen bubbles at the mild steel electrode, leading to sluggish detachment of hydrogen bubbles from its surface.

The added As_2O_3 in the $KF \cdot 2HF$ melt becomes slowly reduced at the electrode surface to elemental As and further to AsH_3. *Ex situ* XPS examination confirmed the presence of As species on or in the top layers of the electrode surface.

Acknowledgement

This work was jointly supported by Natural Sciences and Engineering Research Council of Canada and Cameco Inc., Saskatoon. L J. Gao acknowledges the award of the Joseph Richards Summer Fellowship of the Electrochemical Society held during execution of part of this work. We also acknowledge frequent useful discussions with Drs D. G. Garratt of Cameco Corporation and T. Zawidzki during the course of the work.

References

[1] L. J. Gao and B. E. Conway, *Electrochim. Acta* **39** (1994) 1681.
[2] S. Y. Qian and B. E. Conway, *J. Appl. Electrochem.* **24** (1994) 195.
[3] L. J. Gao and B. E. Conway, *J. Electroanal. Chem.* **395** (1995) 261.
[4] J. O'M. Bockris and B. E. Conway, *Trans. Faraday Soc.* **45** (1949) 989.
[5] P. Marcus and E. Protopopoff, *Surf. Sci.* **17** (1985) 533; see also *J. Electrochem. Soc.* **135** (1988) 3073.
[6] J. Clavilier, J. M. Feliu, A. Fernandez-Vega and A. Aldaz, *J. Electroanal. Chem.* **294** (1990) 193.
[7] J. W. Schultze and F. D. Koppitz, *Electrochim. Acta* **21** (1976) 327.
[8] P. Stonehart and G. Kohlmayr, *ibid.* **17** (1972) 369.
[9] J. O'M. Bockris, J. McBreen and L. Nanis, *J. Electrochem. Soc.* **112** (1965) 1125.
[10] P. K. Subramanyam, in 'Comprehensive Treatise of Electrochemistry', Vol. 4 (edited by J. O'M. Bockris, B. E. Conway, E. B. Yeager and R. E. White), Plenum Press, New York (1981) p. 411.
[11] B. E. Conway and G. Jerkiewicz, *J. Electroanal. Chem.* **357** (1993) 47.
[12] E. Gileadi, E. Kirowa-Eisner and J. Penciner, *in* 'Interfacial Electrochemistry, Addison-Wesley, New York (1975) chapter 7.
[13] A. N. Frumkin, *in* 'Advances in Electrochemistry and Electrochemical Engineering', Vol. 1 (edited by P. Delahay), Interscience, New York (1961) p. 65.
[14] D. A. Harrington and B. E. Conway, *J. Electroanal. Chem.* **221** (1987) 1.
[15] L. J. Gao, S. Y. Qian and B. E. Conway, *J. Appl. Electrochem.* **25** (1995) 6.
[16] L. Bai and B. E. Conway, *J. Chem. Soc., Faraday Trans.* **81** (1985) 1841.
[17] M. C. Sneed and R. C. Brasted, 'Comprehensive Inorganic Chemistry', Vol. 5, D. Van Nostrand, Princeton, NJ (1956) p. 116.
[18] A. J. Rudge, *in* 'Industrial Electrochemical Processes' (edited by A. T. Kuhn), Elsevier, Amsterdam (1971) chapter 1.
[19] G. H. Cady, *J. Amer. Chem. Soc.* **56**(7) (1934) 1431.
[20] B. E. Conway, J. O'M. Bockris and H. Linton, *J. Chem. Phys.* **24** (1956) 834.
[21] M. Eigen and L. de Maeyer, *Z. Elektrochem.* **60** (1956) 1037.
[22] E. Gileadi and B. E. Conway, *J. Chem. Phys.* **39** (1963) 3420.
[23] L. Bai, *J. Electroanal. Chem.* **355** (1993) 37.
[24] A. N. Frumkin and B. Slygin, *Acta Phisicochimica, URSS* **3** (1933) 791.